Voltage-Dependent Formation of Gramicidin Channels in Lipid Bilayers

John Sandblom, Juris Galvanovskis, and Barbro Jilderos
Department of Medical Biophysics, Göteborg University, 40530 Göteborg, Sweden

ABSTRACT The formation kinetics of gramicidin A channels in lipid bilayer membranes has been characterized as a function of voltage for different solution conditions and membrane composition. The frequency of channel events was measured during the application of voltage ramps and counted in given intervals, a procedure that eliminated the effects of drift in gramicidin concentration. The formation rate was found to increase strongly with voltages up to ~50 mV and then to level off slightly. The shape of the voltage dependence was independent of lipid solvent and ramp speed but differed for different ions and different solution concentrations. This suggested an ion occupancy effect on the formation rate that was further supported by the fact that the minimum of the formation rate was shifted toward the equilibrium potential in asymmetric solution concentrations. The effects are explained in terms of a model that contains two contributions to the voltage dependence, a voltage-dependent ion binding to the monomers and a polarization of monomers by the applied electric field and by the occupied ions. The theory is found to give a good fit to experimental data.

INTRODUCTION

Since the reports that gramicidin A forms channels in lipid bilayers (Hladky and Haydon, 1972) by means of a head-to-head dimerization (Urry et al., 1971), a considerable amount of work has been done to characterize the conductance and selectivity properties of these channels. Most of this literature is reviewed in the articles by Woolley and Wallace (1992) and by Busath (1993). Less attention, however, has been paid to the kinetics of formation and dissociation of the conducting units, although a few systematic studies of the lifetime properties of gramicidin A have been made. The first report by Kolb and Bamberg (1977) demonstrated a strong dependence on ion concentration of both lifetime and formation rate. Neher and Eibl (1977) showed that the lifetime correlated with lipid surface tension over a very wide range of values, suggesting that surface tension may be the major factor governing channel lifetimes. Elliot et al. (1983) went further and developed a model that also incorporated membrane thickness and that accounted for the lifetime behavior in membranes of different compositions. Ring and Sandblom (1988a,b) and Ring (1992) studied the concentration dependence of the lifetime and proposed a model that took into account the effects of ion occupancy on the stabilization of the dimer complexes. This model was able to explain the lifetime dependence on concentration and voltage as well as the ion species dependence (Ring and Sandblom, 1988b). Channel lifetimes of gramicidin A have also been used as indicators to study the mechanical properties of lipid bilayer membranes under tension and deformation (Ring, 1996; Goulian et al., 1998; Lundbœk and Andersen, 1999).

Received for publication 5 September 2000 and in final form 24 April 2001.

Address reprint requests to Dr. John Sandblom, Göteborg University, Department of Medical Biophysics, Box 433, 40530 Göteborg, Sweden. Tel.: 46-31-773-3551; Fax: 46-31-773-3558; E-mail: sandblom@mednet.gu.se.

0006-3495/01/08/827/11 $2.00

Regarding the formation kinetics, Bamberg and Läuger (1973) and Bamberg and Benz (1976) used the voltage dependence of the formation rate to study the kinetics after steps in applied voltage. By this method, they were able to measure separately the formation and dissociation rates for a few applied voltages. A more systematic study of the formation rate is still lacking, however, mainly due to the difficulties involved in obtaining stationary recordings. The problem arises because the concentration of gramicidin in the membrane is not constant, but is subject to fluctuations because it exchanges with the torus of the bilayer, and, to some extent, also with the aqueous phases. However, the gramicidin molecules do not cross the membrane in their monomeric form as concluded by O'Connell et al. (1990) in adding different homologues to the two sides of the membrane. They concluded that, whereas the monomeric form of gramicidin could not cross the membrane, a small percentage may appear in a dimeric intertwined form that could flip across the membrane and give rise to channels.

The processes leading to the formation of conducting channels from the predominantly monomeric forms of gramicidin in lipid bilayers may be considered to be composed of four different kinetic steps (see Fig. 1), namely, 1) the partitioning of peptide monomers between the lipid torus (the aqueous solutions in case the gramicidin is added in an ethanol suspension) and the membrane, 2) the subsequent conformational changes of the peptide molecules yielding, as the end result, a helical structure that extends from the interface about half way into the membrane, 3) the diffusion of monomers to a position where they may join, and finally, 4) the hydrogen bonding of two monomers opposite each other to form the dimerized channel. It is not known which of the steps in Fig. 1 that is rate limiting, but the overall process is influenced by several factors such as the applied electric field, the membrane composition, and the external solution conditions.

We have found that these factors can be studied in a systematic way with applied repeated voltage ramps be-

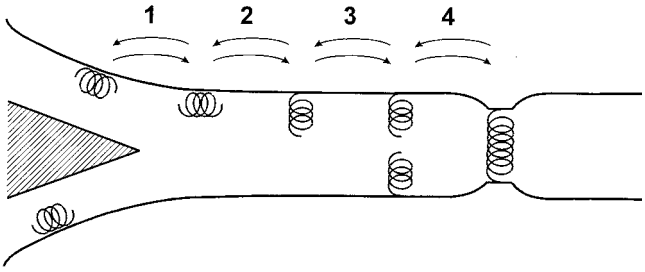

FIGURE 1 Kinetic steps of gramicidin channel formation showing (*1*) the absorption of gramicidin either from the lipid torus or the aqueous phase to the membrane interface, (*2*) the entry of monomers into the membrane, (*3*) the diffusion of opposite monomers to juxtapositions, a process that depends on attraction and repulsion forces between the monomers, and (*4*) the formation of conducting dimers. The gramicidin molecules are schematically represented as helical coils, although it is only in the dimerized form that this structure is verified.

cause drifts due to changes in monomer concentration can be averaged out over a large number of ramps. We find with this method that the formation rate is strongly voltage and concentration dependent, and we propose a model based on channel occupancy and monomer polarization to account for these effects.

METHODS

Bilayer formation

Bilayers were formed using the technique of Neher et al. (1978), later modified by Bokvist and Sandblom (1992), by which a membrane is painted across a hole (100–250 μm in diameter) made in a plastic syringe. The syringe is mounted on the head stage of a current-to-voltage converter. A grounded silver chloride electrode is concentrically arranged around the plastic syringe to provide an effective electric shielding. Gramicidin was generally added to the lipid before membrane formation.

Chemicals

Membranes were made from glycerolmonooleate (GMO) in either decane or hexadecane (14 mg/ml). Decane, hexadecane, and GMO were purchased from Sigma-Aldrich (Sweden). Gramicidin A was purified from a stock solution of gramicidin D (Sigma), which contained a mixture of A, B, and C. The purification was carried out by reversed-phase High Performance Liquid Chromatography (HPLC) according to the method of Koeppe and Weiss (1981). Aqueous solutions of different compositions (Cs, K, Tl, and H) and concentrations were used, and, in all cases, $MgCl_2$ was present at a concentration of 1 molar to reduce large differences in ionic strength between solutions.

Electrical measurements

The voltage was applied across the membrane using triangle-shaped ramps (Fig. 2). The periods of the ramps were set at values between 1 and 5 min, a time interval that is long compared to the channel lifetime but sufficiently short in comparison with drifts in channel activity. With periods within this interval, the results were found to be independent of ramp speeds (see below). The peak values of the ramp were either $\pm$200 or $\pm$100 mV depending on the desired resolution of events. The lower peak amplitude of the ramp allowed a higher amplification to be used and hence a better resolution in counting channel events.

The main limit of accuracy is the detection of channel events near zero voltage. We found, however, that, even if a channel "opening" was too small to be detected, the channel usually stayed open long enough for its "closing" to be seen. Very few events were therefore missed using this procedure, although the values in those intervals that include or border on zero current are likely to be underestimated.

The signal was filtered at 25 Hz before sampling, which we found to give a good detection of small events. With an average lifetime of 1 s, ~1% of the events became undetectable by this filtering.

The ramp was divided in either 10- or 20-mV intervals (see Fig. 2) and the number of events was counted in each interval and subsequently added over many ramps. No distinction was made between increasing or decreasing ramps, i.e., all intervals corresponding to a particular voltage (the midpoint of the 10- or 20-mV interval) were added regardless of whether they were located on increasing or decreasing ramp slopes. Each experiment was carried out over a sufficiently long time to collect at least 100 events in each interval.

The effect of the field on the membrane torus produced a slight variation in membrane area in response to the changing voltage, maximally ~10%. To correct for this effect, the channel formation frequency was normalized with respect to the area obtained by measuring the membrane capacitance during the applied ramp. The capacitance measurements were carried out a couple of times during the course of the experiment by adding a high frequency (100 Hz, 20 mV peak to peak) triangular signal to the ramp and

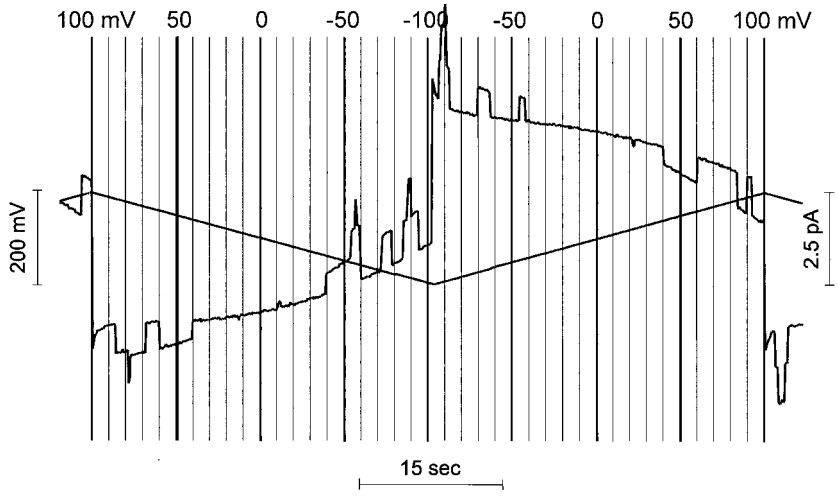

FIGURE 2 Triangle-shaped voltage ramps and corresponding membrane current. The horizontal lines represent intervals in which the channel events are counted.

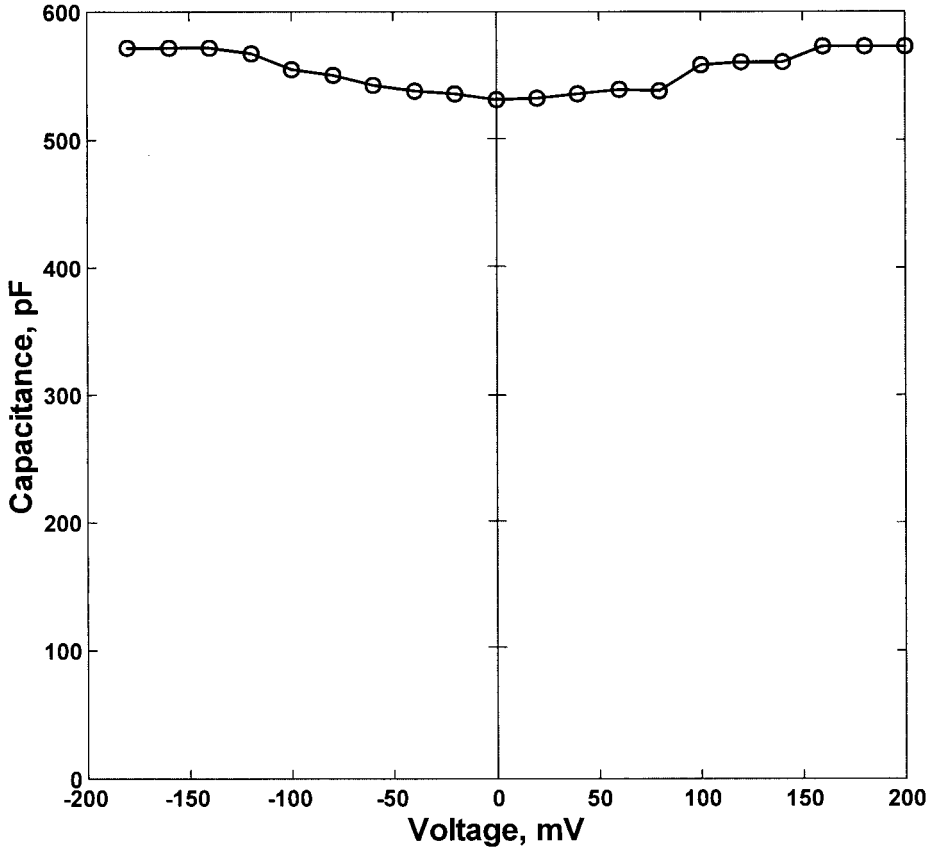

FIGURE 3 The membrane capacitance as a function of voltage in 1 M KCl.

calculating the capacitance from the current steps. Figure 3 shows the result of such a capacitance measurement for the case of 1 M KCl.

There is, in addition to area changes, a contribution to the capacitance variation with voltage (Fig. 3) resulting from a compression of the bilayer by the electric field. However, this is a small and systematic variation. By dividing the formation rates at each voltage by the capacitance, we therefore introduce a small systematic error, but we eliminate the component of variability that is caused by area changes.

To be able to superimpose data from the same solution concentrations but with different ramps (±200 and ±100 mV), we devised a method using a polynomial fit to the data. The data of each experiment were fitted to a polynomial of the type

$$Y = \frac{a_0 + a_1X + a_2X^2 + a_3X^3 + a_4X^4}{1 + bX^2}, \qquad (1)$$

where the coefficients of the odd terms were set to zero in experiments with symmetrical solution conditions. The polynomials corresponding to the different ramp experiments were scaled, and the simultaneous fitting to both experiments gave the scaling coefficients and the polynomial coefficients. A further restriction on the scaling was introduced by setting the formation rate to unity at +50 mV. This normalization eliminates differences in formation rates due to differences in gramicidin concentration among the different experiments. As an example, Fig. 4 shows two sets of data for 0.1 M cesium chloride (±200 and ±100 mV ramps) with the curve obtained by the fitting procedure described above.

A control experiment was made to check that the formation rate was independent of ramp speed for speeds between 10 and 100 mV/min. Figure 5 shows three sets of data for 0.3 M KCl corresponding to different ramp speeds. There is no significant difference in shape between the lower ramp speeds, but, at higher ramp speeds (75 mV/min), there is a slight increase in steepness of the curve. A possible source of this time-dependent component could be the diffusion of gramicidin in and out of the torus (step 1, Fig. 1.) and which does not reach a steady state during the area changes produced by the ramps. At lower ramp speeds, this effect becomes negligible, and, in all of the following experiments, a ramp speed of 25 mV/min has therefore been used.

RESULTS

Figure 6 shows the dependence on voltage of the formation kinetics for three different ions at the same concentration level, Tl, H, and K. A transition from a steep voltage dependence at low voltages to a lesser dependence at higher voltages, and which is explained by the theory put forth below, is seen in all cases. The voltage dependence is also, to some extent, species dependent. Tl and K do not differ greatly (see also Fig. 9 *A*), whereas the voltage dependence in H has a slightly different shape (see also Fig. 9 *B*).

Figure 7, *A–C*, shows the behavior at different concentrations of KCl, and the increase in formation rate between 0 and 100 mV is seen to be largest in 0.1 M KCl and smallest in 1 M KCl. Figure 8 shows data for two different lipid solvents, decane and hexadecane, in solutions of 0.01

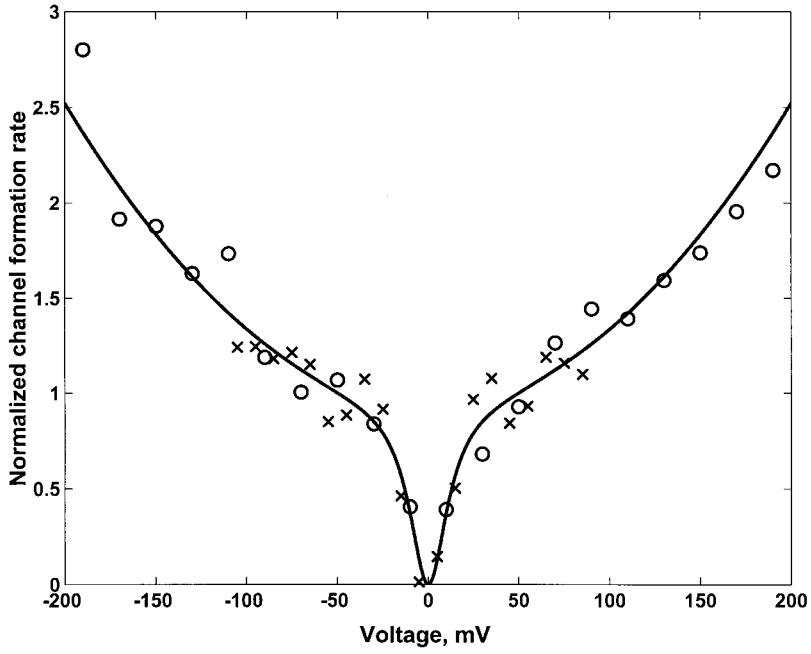

FIGURE 4 The formation rate in symmetrical solutions of 0.1 M CsCl + 1 M $MgCl_2$ for ±200 mV ramps (○) and ±100 mV ramps (×). The line is obtained from the curve-fitting procedure described in the text.

M KCl. The curves deviate at higher fields where the effect may be a direct influence on the lipid membrane. The negligible difference between the curves at lower voltages suggests that the observed voltage dependence in this range is the result of a direct effect of the field on the peptide rather than on the membrane.

Figure 9 shows the voltage dependence of the formation rate in asymmetric solutions, (*A*) 0.01 M TlCl//0.01 M KCl and (*B*) 0.1 M HCl//0.1 M KCl. The minimum in the formation rate is seen to occur approximately at the equilibrium potential of the system, although the shapes of the curves are seen to be highly species dependent. The formation rate at positive voltages when H^+ is driven into the membrane is significantly lower than when K^+ is driven into the membrane (see Fig. 9 *B*). The difference between the ions is seen to be much less in the Tl^+-K^+ case (Fig. 9 *A*).

The concentration dependence on the formation rate and the shift in minimum toward the equilibrium potential in asymmetric solutions suggest that ion occupancy is impor-

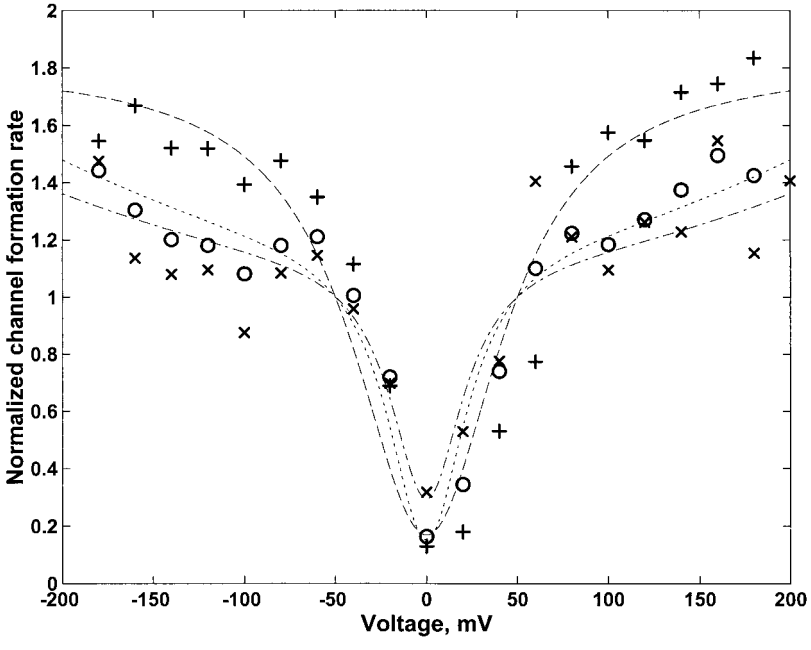

FIGURE 5 The formation rate in 0.3 M KCl + 1 M $MgCl_2$ at 3 different ramp speeds, (+) 75 mV/s, (○) 7 mV/s, and (×) 25 mV/s.

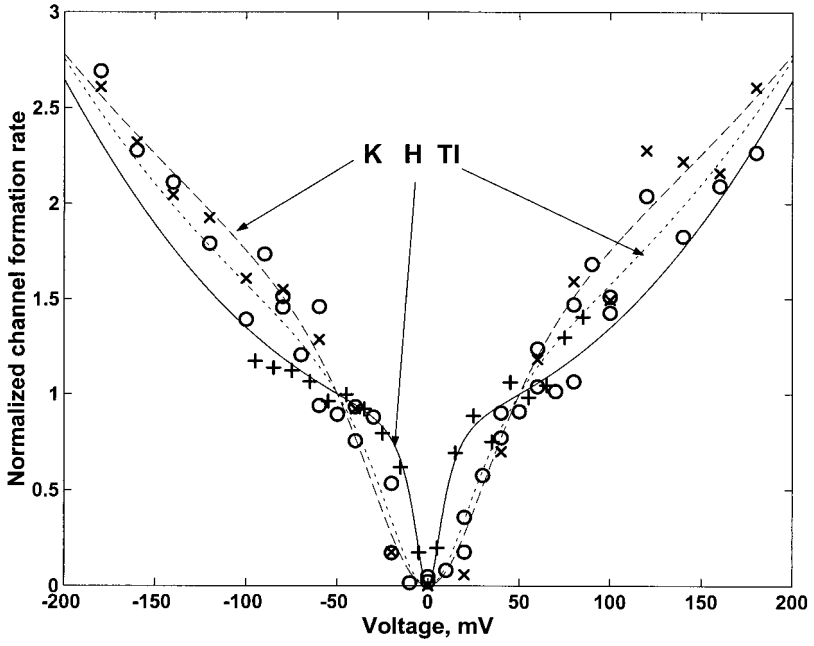

FIGURE 6 The formation rate in 0.01 M KCl + 1 M $MgCl_2$ (×, *dashed line*),0.01 M TlCl + 1 M $MgCl_2$ (○, *dotted line*), and 0.01 M HCl + 1 M $MgCl_2$ (+, *solid line*).

tant in regulating the formation rate. However, the steepness of the voltage dependence at low voltages is not sufficiently explained by the location of an ion binding site inside the peptide monomer where the bound ion senses the electric field. We suggest that the peptide monomer is directly polarized by the field, thereby shifting the energy of interaction between the monomers, to account for the steepness. The model we have examined is based on the Langevin dipole concept used by Åquist and Warshel (1989) to calculate internal energy profiles for ion binding. We will use this to calculate an average energy of interaction between monomers in the two halves of the membrane.

THEORY

Model

The model of the membrane including the helical monomers and penetrating ions is shown in Fig. 10. Two factors contribute to the polarization of the monomers (indicated as polarized water molecules), the externally applied field and the internal field generated by the occupied ions. The rate constants for dimerization in the different configurations are indicated in the figure. The monomers are assumed to be in the same conformation as in their dimerized form, and their concentration is further assumed to remain constant in the membrane, i.e., we assume the rates of exchange with the surroundings to be small compared with the association and dissociation rates.

We shall limit the treatment to the case of low dimer concentration, in which case the gramicidin molecules in each half of the membrane exist primarily in two monomer states (empty ○ or occupied by an ion ×). The rate of formation of channels depends on the occupancy states of the monomers, and the net rate is given by the sum of the individual rates for each occupancy state,

$$\begin{aligned} \mathrm{FR} = {} & k_0 \cdot P(\bigcirc)' \cdot P(\bigcirc)'' \\ & + k_1 \cdot (P(\times)' \cdot P(\bigcirc)'' + P(\bigcirc)' \cdot P(\times)'') \\ & + k_2 \cdot P(\times)' \cdot P(\times)'', \end{aligned} \tag{2}$$

where k_0, k_1, and k_2 are the rate constants for dimerization in the combined occupancy configurations ○○, ×○ + ○×, and ××, respectively (see Fig. 10). The probabilities that the monomers are unoccupied or occupied are denoted by $P(\bigcirc)$ and $P(\times)$ and the superscripts $'$ and $''$ refer to the two sides of the membrane. The occupancy probabilities are related through equations for binding of ion × to the monomers

$$\begin{aligned} P(\times)' &= C_x' \cdot \exp(f \cdot U) \cdot P(\bigcirc)' \cdot K_x, \\ P(\times)'' &= C_x'' \cdot \exp(-f \cdot U) \cdot P(\bigcirc)'' \cdot K_x, \end{aligned} \tag{3}$$

where K_x is the binding constant, f the fraction distance along the potential gradient of the binding site location, and U is the membrane potential normalized with respect to RT/F.

Combining Eqs. 2 and 3 gives an expression for the formation rate in terms of the applied voltage,

$$\mathrm{FR} = \frac{\begin{array}{c} k_0 + k_1 \cdot K_x \cdot (C_x' \exp(f \cdot U) \\ + (C_x'' \exp(-f \cdot U)) + k_2 \cdot K_x^2 \cdot C_x' C_x'' \end{array}}{\begin{array}{c} (1 + K_x C_x' \exp(f \cdot U)) \\ \cdot (1 + K_x C_x'' \exp(-f \cdot U)) \end{array}} \tag{4}$$

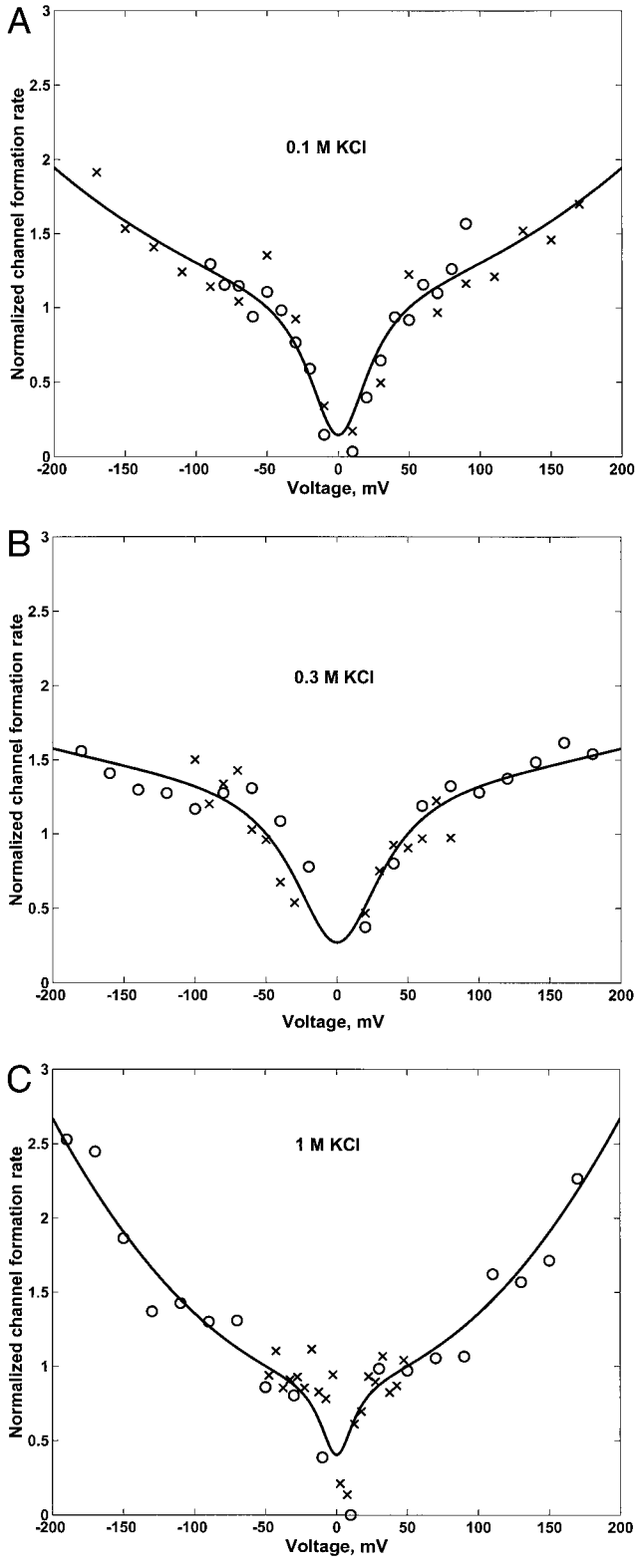

FIGURE 7 The formation rate for KCl at three different concentrations: (*A*) 0.1 M, (*B*) 0.3 M, and (*C*) 1.0 M. 1 M $MgCl_2$ was added to each side in the experiment.

Eq. 4 expresses an explicit voltage dependence that originates from the species-dependent occupancy effect. However, the rate constants in the above expression also depend, in general, on the applied voltage, and, although several mechanisms may contribute to this, we will consider here only the effect of polarizing the monomers because this produces a very strong voltage dependence. Such a polarization will be generated by the applied electric field, which, in orienting the dipoles of the peptide and the water molecules, will give rise to a net dipole moment of each monomer. However, the orienting force E_{tot} will not only consist of an externally applied field E_{appl} but also of an internal force E_{int}, generated by the occupying ions, and we get, for the total polarizing energy U_{tot},

$$U_{tot} = U_{appl} + U_{int}. \tag{5}$$

We shall write an expression for the internal force by viewing the charges of the ion-occupied monomers as an average surface charge smeared out on a plane inside the bilayer. This is a valid physical picture if the movement of charges in and out of the membrane are fast compared to other processes affected by the internal force, for instance, the polarization of monomers and the dimerization process. In the following treatment, this picture will be used as a first-order approximation of the detailed dynamics of the system. We will therefore derive an expression for the internal force based on this surface-layer approximation of the charge distribution of the ion-occupied monomers. The surface charge density of the internal layer is proportional to the ion occupancy, and the net internal force can therefore be written in terms of an internal potential that is proportional to the difference in ion occupancy of the opposite monomers,

$$U_{int} = A \cdot (P(\times)' - P(\times)''), \tag{6}$$

where A is a constant that depends, in general, on the monomer density, on the location of the binding sites, and on the dielectric constant of the membrane. It should be emphasized that Eq. 6 contains only the contribution of the occupied ions to an average overall monomer polarization and does not contain any specific ion dipole interactions. These specific interactions are instead incorporated in the rate constants of Eq. 2.

The net dipole moment of each monomer is now derived from the Langevin function, which incorporates the opposing effect of thermal agitation on the tendency of the dipoles to line up with the polarizing field. A physical treatment of this effect yields a function $\mathcal{L}(x)$, derived by Langevin, for the net polarization of the monomers as a function of their dipole moments and polarizing force. It is given by

$$£(x) = \coth x - 1/x, \tag{7}$$

which is a very steep function near $x = 0$, but levels off and approaches unity when x tends toward infinity. A derivation

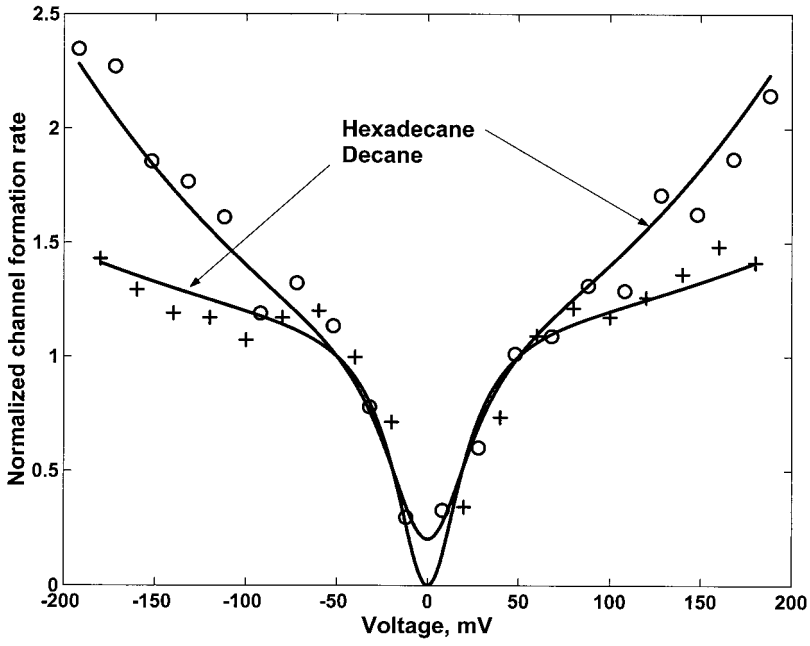

FIGURE 8 The voltage dependence of the formation rate in two different solvents: (+) decane and (○) hexadecane. The bathing solutions were 0.3 M KCl + 1 M $MgCl_2$.

of this function is found in standard textbooks (see, for instance, Atkins, 1982, p. 71).

We write the Langevin function for the dipole moment of the monomers as $\mathcal{L}(0.5pU_{tot})$, where p is a number expressing the number of charges moved along the monomer in polarizing it. This function is used to compute the energy of interaction between two opposite monomers due to polarization and which is proportional to the square of the individual dipole moments. The energy of interaction is therefore equal to $Bp^2\mathcal{L}^2(0.5pU_{tot})$, where B is a constant that depends on the mean distance between the monomers and the dielectric constant of the membrane.

Using this interaction term, we can now write expressions for the explicit voltage dependence of the rate constants appearing in Eqs. 3 and 4,

$$k_i = k_i^0 \cdot \exp\left(Bp^2 \cdot \mathcal{L}^2\left(\tfrac{1}{2}pU_{tot}\right)\right) \tag{8}$$

where k_i^0 are the voltage-independent parts of the rate constants. Finally, by combining Eqs. 8 and 4, we get the desired expression for the formation rate. Apart from a scaling factor, this expression is seen to contain eight independent parameters (A, B, p, f, K_x, k_0^0, k_1^0, k_2^0) to be determined from experimental data.

Fit to experimental data

An estimate of the parameters is made by fitting the model to the data in asymmetric solutions of the same ion. Figure 11 shows a fit of the model to an asymmetric case of KCl, 10/1 in concentration. In fitting the model to the data of Fig. 11, we put $k_2 = 0$ by assuming that the electrostatic repulsion between oppositely occupied monomers will reduce the dimerization tendency. This fit of the model to the data of Fig. 11 was carried out using a routine in the software package MATLAB.

The result of the fit (Fig. 11) gave the following values of the parameters: $A = 6.5 \cdot 10^4$ (in units of RT/F), $B = 0.28$ (in units of kT), $p = 4.3$, $f = 0.39$, $K_x = 1.9 \cdot 10^{-4}$ M^{-1}, $k_0^0 = 0.03$ s^{-1} and $k_1^0 = 4.1$ s^{-1}. The model function fits very well to the experimental data over the whole range of voltages. The iterative procedure converged to a final set of parameter values, indicating that a minimum of the objective function was found.

The fitting curves are most sensitive to changes in the parameter f. A 10% decrease in the value of this parameter greatly diminishes the channel formation rate. The convergence of the fit is also sensitive to the product $A \cdot K_x$, although less sensitive to A and K_x individually. The shape at low voltages determines the parameters of the Langevin function (A, B, and p), whereas the shape at higher voltages determines the occupancy parameters (K_x, k_0^0 and k_1^0).

The parameters of the fit in Fig. 11 were used to calculate a set of curves for the concentrations used in the experiments shown in Fig. 7, *A–C*. The calculated curves and the experimental data are shown in Fig. 12, which shows a good agreement between the predictions of the model and the experimental data. The theory also explains the bimodal appearance of the data where the dipolar interactions are responsible for the steepness at low voltages and where the ion occupancy effects predominate at higher voltages where the Langevin function has leveled off.

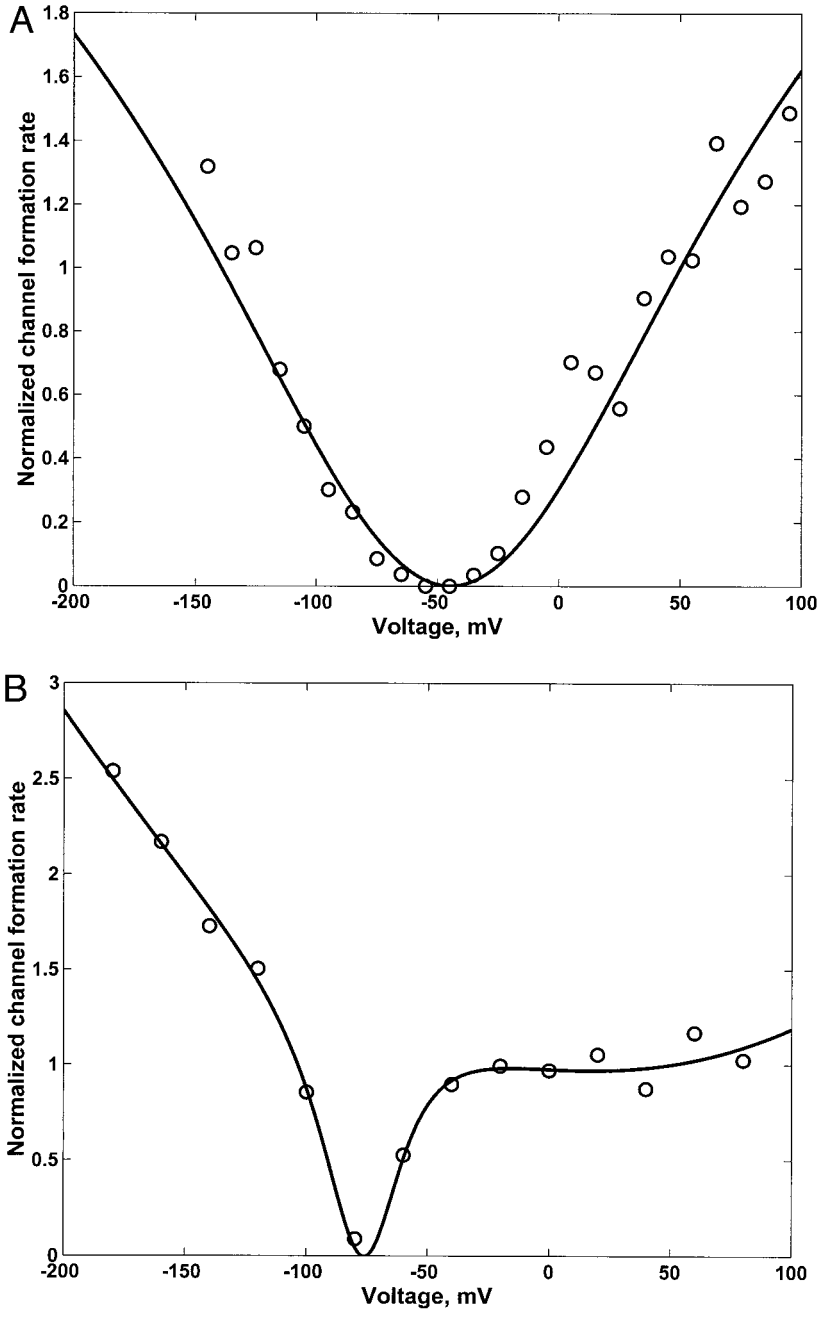

FIGURE 9 The formation rate in asymmetric solutions (*A*) 0.01 M TlCl + 1 M $MgCl_2$//0.01 M KCl + 1 M $MgCl_2$ and (*B*) 0.1 M HCl + 1 M $MgCl_2$//0.1 KCl + 1 M $MgCl_2$.

DISCUSSION

The parameter values produced by the fit may be examined from a physical point of view. The value of f (0.4) implies that the binding site for the ion is located nearly at the inner end of the monomer. The low binding constant ($1.9 \cdot 10^{-4}$ M^{-1}) is a logical consequence of this. In the dimerized channel, the binding site is shifted outward and the binding constant is several orders of magnitude higher. A comparison between the rate constants k_0^0 and k_1^0 shows that the formation rate is much higher (~100 times) when an ion occupies the monomer than when the monomers are empty. This is a clear indication of the polarizing effect that an ion exerts on opposite monomers.

The value of p is 4.3, which means that the equivalent of about 4 charges move along the monomer when it polarizes. This gives a value for the dipole moment of the monomer of ~300 Debye, which is two orders of magnitude higher than the dipole moments of the individual amino acids and water molecules constituting a monomer. This is a high value even when taking into account that several amino acids and water molecules contribute to the overall polarization of the gramicidin molecules. We have therefore examined the possibil-

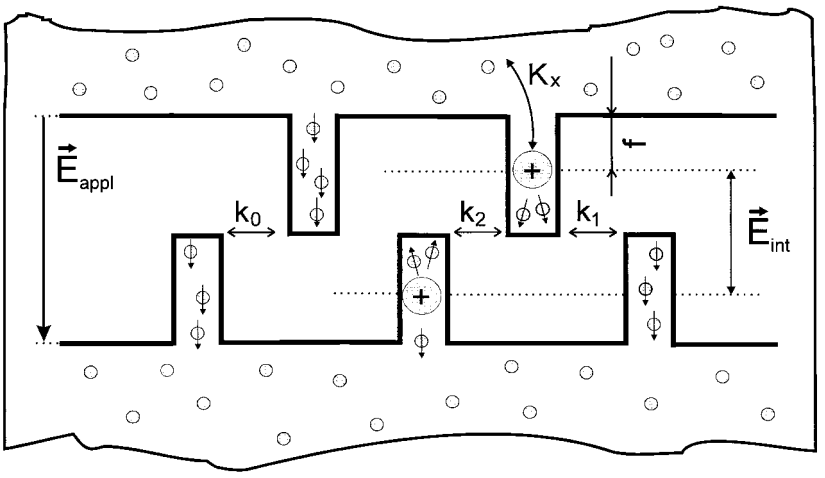

FIGURE 10 Model of the membrane showing the various interaction forces between monomers. The figure shows the polarization of water molecules under the influence of internal and applied fields. The parameters of the model, defined in the text, are shown in the figure.

ity to restrict the values of p and A in making the computations. By keeping p less than unity and the value of A (to which the unconstrained fit also assigns a high value) to less than 100, the algorithm finds a minimum which still gives a very good fit to the data without qualitatively altering the remaining parameters. Further restricting A and p, however, gradually destroys the goodness of the fit. A value of p that is unity now implies that one charge is moved along the monomer in polarizing it, which gives a value of 70 Debye for the dipole moment of the monomer.

To discuss the meaning of the A value, we note that this parameter expresses the force exerted by the ionic charge on the neighboring monomers. We can therefore get an estimate of the Coulomb force by computing the distance away from the occupied ion where the potential assumes the value of 100 (in units of RT/F). Using Coulombs law and a value of the dielectric constant of 2 we obtain a value of 3 Å for this distance, which implies that the ionic charge has a very close range of action on the polarized monomer during the formation of the channel.

In conclusion, by constraining the values of A and p, it is possible to obtain a good fit of the model to the data within the framework of a reasonable physical model. However, because the unconstrained fit of the model assigns very high values to A and p, which are responsible for the steepness in shape, this may also indicate that other voltage-dependent processes, not incorporated in the theory, may be involved in the dimer formation by gramicidin monomers inside bilayer membranes, for instance aggregation of monomers or the variation of membrane thickness.

The strong voltage dependence of the formation rate of gramicidin channels, which increases by about a factor of 10

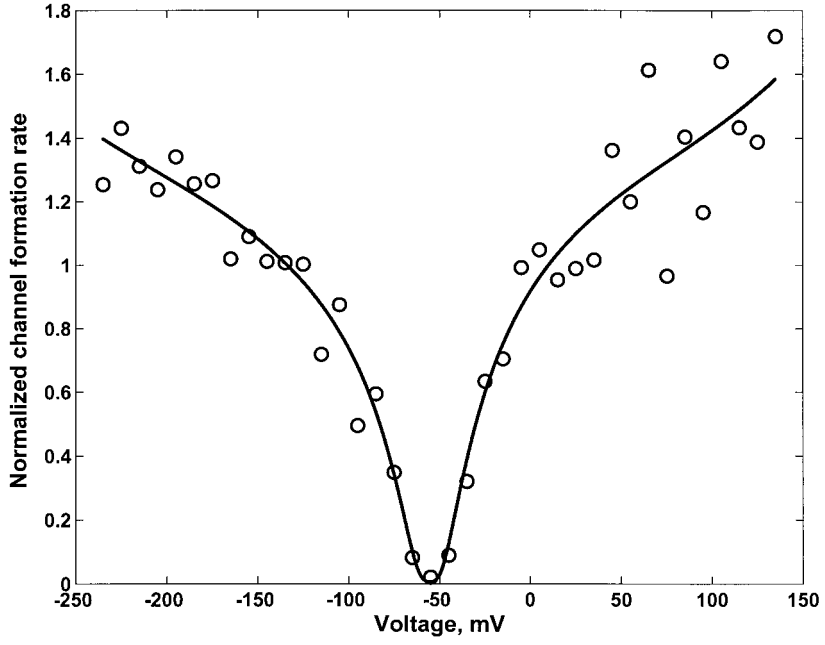

FIGURE 11 Fit of the model, Eqs. 4 and 8, to asymmetric data of KCl (0.01 M KCl + 1 M $MgCl_2$//1 M KCl + 1 M $MgCl_2$). The fit is made using a simplex algorithm (MATLAB) and the parameters obtained are $A = 6.5 \cdot 10^4$ (in units of RT/F), $B = 0.28$ (in units of kT), $p = 4.3$, $f = 0.39$, $K_x = 1.9 \cdot 10^{-4}$ M^{-1}, $k_0^0 = 0.03$ s^{-1}, and $k_1^0 = 4.1$ s^{-1}.

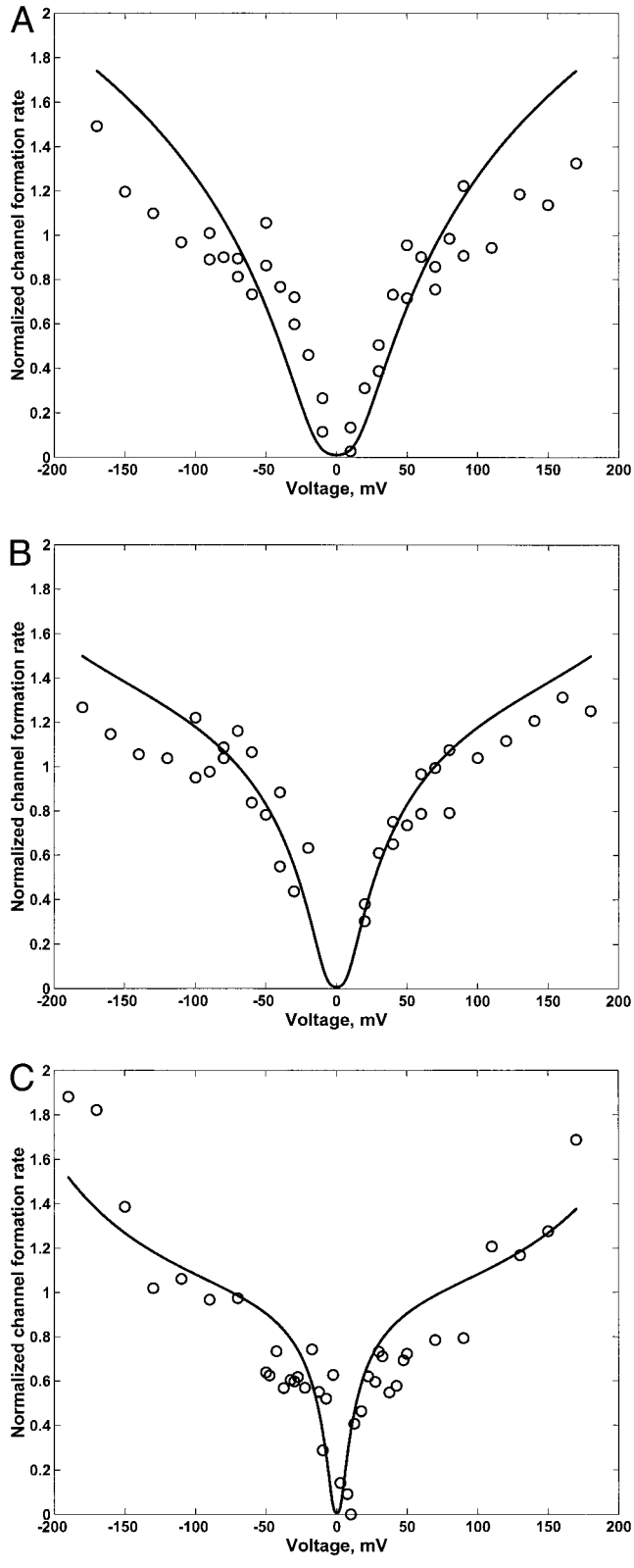

FIGURE 12 The model prediction for different concentrations are calculated using the parameters given in the legend of Fig. 11. The experimental data are the same as those of Fig. 7, *A–C*, although scaled to the theoretical curves.

between 0 and 200 mV, has also been observed by previous investigators. Bamberg and Läuger (1973) reported such a strong voltage dependence from their voltage jump experiments and arrived at a six-fold change in formation rate between 0 and 200 mV. However, their value at 0 voltage was estimated by extrapolation, and it is clear from their figure that the formation rate at zero voltage should be considerably lower, which would be in agreement with our results.

From the data of Bamberg and Läuger, it was also concluded that the voltage dependence of formation starts decreasing at conductances above 10^{-6} S/cm^2 due to the increase in dimer to monomer ratio. Because the amount of gramicidin in the membrane is fixed, the dimer concentration at high gramicidin levels reaches saturation, and, at this point, the formation rate approaches a constant. The voltage dependence of the formation rate is therefore expected to decrease at high gramicidin levels, which we have verified in experiments approaching many channel events (unpublished results).

Although the voltage jump experiments of Bamberg and Läuger provide a way for exact measurements of the formation rate, the voltage ramp experiments presented here are more sensitive near zero voltages and is a more direct way to obtain a continuous set of values as a function of voltage.

As mentioned above there may be other mechanisms responsible for the observed strong voltage dependence of the formation rate than the one presented here. One possibility could be that the field acts by changing the membrane thickness, which would change the distance between the monomers and alter the barrier for dimerization. However, the slight difference in behavior between hexadecane and decane membranes suggests that the effects on lipid thickness is of less importance for the voltage dependence.

Another mechanism that would give a voltage dependent formation rate has been proposed by Urry (1972), namely that the monomers exist in two conformations with only one of them having the ability to form conducting dimers. If the channel-forming conformation has a higher dipole moment, the applied field could shift the equilibrium toward this form and favor the dimerization.

The shift in minimum of the voltage curves of the formation rate in asymmetric solutions, however, suggests that ion occupancy may play a role, and we therefore propose that both ion occupancy effects and monomer polarization contribute to the strong voltage dependence of channel formation of gramicidin A.

This work was supported by a grant from the Swedish Medical Research Council (4138).

REFERENCES

Åquist, J., and A. Warshel. 1989. Energetics of ion permeation through membrane channels. Solvation of Na^+ by gramicidin A. *Biophys. J.* 56:171–182.

Atkins, P. W. 1982. Physical Chemistry. Oxford University Press, Oxford.

Bamberg, E., and R. Benz. 1976. Voltage-induced thickness changes of lipid bilayer membranes and the effect of an electric field on gramicidin A channel formation. *Biochim. Biophys. Acta.* 426:570–580.

Bamberg, E., and P. Läuger. 1973. Channel formation kinetics of gramicidin A in lipid bilayer membranes. *J. Membr. Biol.* 11:177–194.

Bokvist, K., and J. Sendblom. 1992. Mechanisms of facilitation and blocking in gramicidin channels by impermeations. *J. Membr. Sci*. 66: 157–168.

Busath, D. 1993. The use of physical methods in determining gramicidin channel structure and function. *Annu. Rev. Physiol.* 55:473–501.

Elliot, J. R., D. Needham, J. P. Dilger, and D. A. Haydon. 1983. The effects of bilayer thickness and tension on gramicidin-channel lifetime. *Biochim. Biophys. Acta.* 735:95–103.

Goulian, M., O. N. Mesquita, D. K. Fygenson, C. Nielsen, O. S. Andersen, and A. Libacher. 1998. Gramicidin channel under tension. *Biophys. J.* 74:328–337.

Hladky, S. B., and D. A. Haydon. 1972. Ion transfer across lipid membranes in the presence of gramicidin A. 1. Studies of the unit conductance channel. *Biochim. Biophys. Acta.* 464:37–44.

Koeppe, R., and B. Weiss. 1981. Resolution of linear gramicidins by preparative reversed-phase high-performance liquid chromatography. *J. Chromatog.* 208:414–418.

Kolb, H., and E. Bamberg.1977. Influence of membrane thickness and ion concentration on the properties of gramicidin A channels. *Biochim. Biophys. Acta.* 464:127–141.

Lundbœk, J. A., and O. S. Andersen. 1999. Spring constants for channel-induced lipid bilayer deformations estimates using gramicidin channels. *Biophys. J.* 76:889–895.

Neher, E., and H. J. Eibl. 1977. The influence of phospholipid polar groups on gramicidin A channels. *Biochim. Biophys. Acta.* 464:37–44.

Neher, E., J. Sandblom, and G. Eisenman. 1978. Ionic selectivity saturation and block in gramicidin A channels. II. Saturation behavior of single channel conductance and evidence for the existence of multiple binding sites in the channel. *J. Membr. Biol.* 40:97–116.

O'Connell, A. M., R. E. Koeppe, and O. S. Andersen. 1990. Kinetics of gramicidin channel formation in lipid bilayers: transmembrane monomer association. *Science.* 250:1256–1259.

Ring, A. 1992. Influence of ion occupancy and membrane deformation on gramicidin A stability in lipid membranes. *Biophys. J.* 61:1306–1315.

Ring, A. 1996. Gramicidin channel-induced lipid membrane deformation energy: influence of chain length and boundary conditions. *Biochim. Biophys. Acta.* 1278:147–159.

Ring, A., and J. Sandblom. 1988a. Evaluation of surface tension and ion occupancy effects on gramicidin A channel lifetime. *Biophys. J.* 53: 541–548.

Ring, A., and J. Sandblom. 1988b. Modulation of gramicidin A open channel lifetime by ion occupancy, *Biophys. J.* 53:549–559.

Urry, D. W. 1972. A molecular theory of ion-conducting channels: a field-dependent transition between conducting and nonconducting conformations. *Proc. Natl. Acad. Sci. U.S.A.* 69:1610–1614.

Urry, D. W., M. C. Goodall, J. D. Glickson, and D. F. Mayers. 1971. The gramicidin A transmembrane channel characteristics of head to head dimerized (L, D) helices. *Proc. Natl. Acad. Sci. U.S.A.* 68:1907–1911.

Woolley, G. A., and B. A. Wallace. 1992. Model ion channels: gramicidin and alamethicin. *J. Membr. Biol.* 129:109–136.